

Design of a capacitive main power coupler for RF superconducting accelerators*

HE Fei-Si(贺斐思)¹⁾ HAO Jian-Kui(郝建奎) ZHANG Bao-Cheng(张保澄) ZHAO Kui(赵夔)

(State Key Laboratory of Nuclear Physics and Technology, Peking University, Beijing 100871, China)

Abstract An updated main coupler has been designed for the superconducting accelerator of Free Electron Laser (FEL) project under construction in Peking University. A capacitive structure is chosen for the main coupler. Numerical investigation using CST Microwave Studio demonstrates the cold window part. The other nonstandard structures such as holding rods and antenna are also optimized. The coupler uses a 95% purity Al_2O_3 ceramic cold window. The VSWR (Voltage Standing Wave Ratio) is 1.02 at 1.3 GHz and the frequency bandwidth is 45 MHz with $\text{VSWR} < 1.1$. The electric field intensity is 8.5×10^{-2} kV/mm around the window with 20 kW Continuous Wave (CW) transmitted power. The Q_{ext} is designed variable from 5×10^6 to 1×10^7 .

Key words coupler, capacitive coupling, cold window, coaxial line, PKU FEL

PACS 29.20.Ej, 84.40.Fe

1 Introduction

Relating to the characteristic of the RF superconducting accelerators, the main coupler has to satisfy the following requirements^[1]: serving as a RF-transparent vacuum barrier, low heat leak and microwave reflection, high average through power, critical coupling to the cavity, easy to manufacture and assemble, reliable performance, etc. All the above requirements make the main coupler a difficulty in the superconducting accelerator field. To improve the performance and reduce the costs, we have designed a new coupler to replace the old one used in the PKU 1.5 cell DC-SC injector. We are confident of the new structure as there has been a report of successful sample^[2].

2 Study of the main coupler

The main coupler is designed for the 3+1/2 cell DC-SC injector^[3] and the 9 cell cavity accelerator^[4] of PKU-FEL facility at Peking University. The structure of 9 cell cryomodule with the main coupler is shown in Fig. 1. The main parameters of the 9 cell cavity accelerator are shown in Table 1.

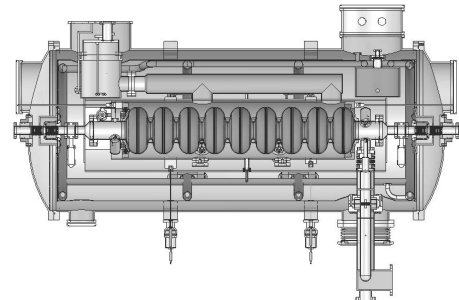


Fig. 1. PKU 9 cell cavity.

Table 1. Parameters of the 9 cell cavity accelerator.

frequency/GHz	1.3
quality factor	1×10^{10}
beam charge/pC	~ 50
repetition frequency/MHz	26
energy spread(rms)(%)	0.24
transverse emittance(rms)/ μm	~ 3
input power/kW	20(CW)
Q_{ext}	$9 \times 10^6 - 1 \times 10^7$
vacuum/Pa	10^{-7} (in cavity)
	10^{-5} (between cold and warm window)

The main coupler consists of three parts, which are sealed by flanges between each other, as shown in Fig. 2. Part one contains the coaxial line, the impedance transformer and the holding rods. It is connected with the beam tube outside the cavity and runs at 2 K to 77 K (liquid nitrogen temperature).

Received 7 September 2007

* Supported by National Basic Research Program (2002CB713600) and NSFC (10775010)

1) E-mail: hef@pku.edu.cn

Part two is the cold window, which is the essential structure. A disc-type ceramic is brazed in the middle of the flange. Part three contains the coaxial line, the holding rods, the “door-knob” and the pumping port. It is connected with the LN₂ cryomodule and warm window.

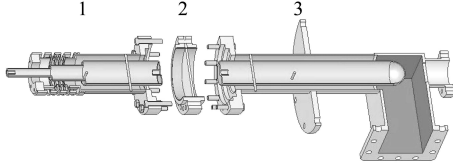


Fig. 2. Structure of the main coupler.

There are three kinds of traditional ceramic windows used in the coaxial lines. One is the cylindrical window, whose two bottoms are both welded with the inner conductor. The other two kinds are disc-like window and conical window, which have holes in their center to be welded with both the inner and the outer conductor. Correspondingly, the capacitive coupling structure has the following notable advantages: 1) the window is a whole disc, which makes it easy to sinter and process, meanwhile the welding seals are reduced from 2 to 1 to guarantee high vacuum and increase stability. 2) As the inner conductor is divided into two parts (note that there are several millimeter’s distance between the inner conductor and the ceramic window), there is less heat exchange with the room temperature part, which may reduce the load of the cryogenic system, especially that of the liquid helium (LHe) system (although the primary heat load still comes from Ohm loss on the surface of the coupler). 3) As some parts of the main coupler work at extremely low temperature, contraction should be taken into consideration. The difference in the coefficient of thermal expansion between metal and ceramic will bring in additional heat stress on the welds and the ceramic window. The axial stress could be ignored due to the separation of inner conductor and window, and actually most radial stress can also be absorbed if properly designed. On the contrary, there is great axial stress on traditional disc-type or conical-type windows, which may increase the risk of window crack. 4) Maybe a key advantage of the coupler is that it is easy to assemble. After a series of polishing and cleaning, the cavity will be assembled with the main coupler, the LHe tank and the cryostat in the clean room, pumped and sealed to keep the cavity clean. Compared with the traditional couplers, only part one and part two shown in Fig. 2 have to be assembled in the clean room instead of the whole coupler. This will not only simplify the assembling and transportation, but also prevent the cold window from deformation stress during assembling.

3 RF design of key structures

3.1 Material for the window

As mentioned above, Ceramic is used as an RF window as well as vacuum barrier. The material must satisfy the following requirements: 1) Low dielectric loss in RF band. 2) High thermal conductivity at low temperature to reduce heat stress caused by temperature gradient. 3) Enough mechanical strength. 4) Low outgassing rate. 5) Easy to process and braze.

The commonly used material is alumina, whose physical properties, especially RF properties, are strongly associated with the purity, sintering binder content, sintering arts and post processing. There are significant differences in all kinds of commercial alumina and samples made in labs. To avoid the damage to the window should be the primary consideration while choosing the material. Specifically^[5, 6], one should reduce the loss tangent, reduce the inner heat source and prevent it from multipacting (MP).

The reduction of loss tangent leads to less heat generation, thus less heat stress caused by temperature gradient. A key method is to reduce the proportion of magnesium sintering binder.

Amorphous MgO or voids in the ceramic may serve as the local heat source, which will cause melting of the ceramic under high transmitted power. Luckily, this effect is not too serious under 20 kW CW power. We have to pay attention to the contradiction between the sintering binder and the voids. For this purpose, it is helpful to use high purity (>99.9%), ultra fine (diameter<0.5 μm) alumina powders, apply Hot Isostatic Processing (HIP)^[5], or apply a two-step sintering^[7].

To protect the window from MP, the common methods include^[6]: 1) to apply a thin film coating of materials with low secondary electron yield (SEY) on the window, e.g. TiN. 2) to destroy the electromagnetic field which supplies MP, for example, to design the structure to make the surface electric field within the range that SEY is less than 1, or to apply an electron field between the inner and outer conductor to destroy the trajectory of MP.

Having considered the requirements above, we chose a 95% alumina window for our first coupler sample, for the sake of reducing the difficulty of brazing of metal and ceramic.

3.2 Optimizations for cold window structure

The cold window has a capacitive structure. The inner conductor is divided into two parts with the ceramic window in the middle, as shown in Fig. 3. The goal of the calculation is to make the microwave reflection minimum near 1.3 GHz by modifying the

geometry parameters.

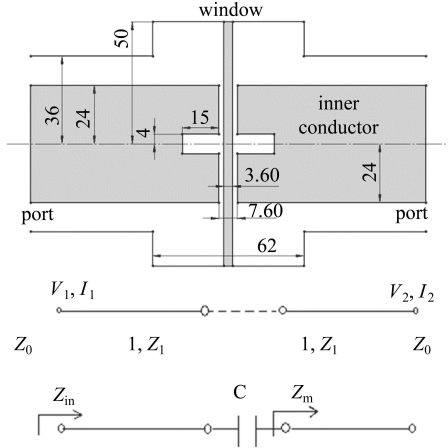


Fig. 3. Schematic section view and equivalent circuit of the cold window.

According to the transmission line theory, we say it is capacitive coupling because the distance between the inner conductors is much less than the wavelength λ ($\lambda=230.6$ mm at 1.3 GHz). The window can be treated as a lumped element capacitor in the equivalent circuit. As the circuit should be resistant when well matched, we can change the characteristic impedance of transmission line near the capacitor to eliminate the effects of the imaginary part introduced by capacitor. This can be achieved by changing the diameter of the outer conductor.

When the outer impedance is matched with the transmission line, the inner impedance Z_{in} meets the following formula^[8]:

$$Z_{in} = Z_1 \frac{Z_m + (j\omega C)^{-1} + jZ_1 \tan \beta l}{Z_1 + j(Z_m + (j\omega C)^{-1}) \tan \beta l},$$

where

$$Z_m = Z_1 \frac{Z_0 + jZ_1 \tan \beta l}{Z_1 + jZ_0 \tan \beta l},$$

Z_1 is the characteristic impedance of coaxial lines near the window, l is the length of transmission line, C is the capacitance, ω and β are the circular frequency and wave number, Z_0 is the impedance of coaxial lines far from the window. Parameters can be determined by solving $Z_{in}=Z_0$. There are no analytical solutions and numerical solution can be applied.

In fact, the shunt capacitor caused by the division should be taken into consideration, and the calculation using equivalent circuit may be quite complex and inaccurate. So the calculation is carried out by the 3D electromagnetic software CST microwave studio 2004. We use the transient solver, which applies integral form Maxwell equations to the model at discrete time and space, to check how the imported energy changes in time domain, and to solve the corresponding eigenvalue equations to obtain a stable field.

The inner conductor uses a thin-wall structure for reducing the weight. Pumping ports are added to both ends of the inner conductor, and a section of tube extends from the pumping ports to serve as microwave cutoff, which can be seen in Fig. 2. When building the calculating model, we treated the inner conductor solid to save time, as the electric field inside the inner conductor is zero. The fillets of 2 mm on the conductor are used to reduce the surface field.

Parameters used in the numerical calculation are as the following: the radial grid spacing is 1 mm, the axial grid spacing is 2.7 mm, the energy accuracy is -60 db (0.1%), the frequency band is 1–1.7GHz. It takes about 8 min for each calculation and the accuracy is acceptable. In addition, we find that the transmission of the higher order modes can be ignored, so we set two magnetic boundary conditions through the rotational symmetry axes. The solving time is reduced to 3 min. From the calculation, we find that the RF properties are not sensitive to the size of pumping ports. For the ceramic, different thickness shows small difference in thermal properties when it is much less than the wavelength, so we set a 3.6 mm thickness taking into account the mechanical strength and heat generation. Then we optimize the capacitor distance d_c , the coupling coaxial length d_{cex} and the outer diameter of coupling coaxial r_{ex} , using the CST build-in optimization function, which sets a function $F(\text{var})=S_{11}(\text{var})-S_{11\text{goal}}$ and solves $F(\text{var})=0$ with Newton root law. Here S_{11} is the voltage reflecting rate.

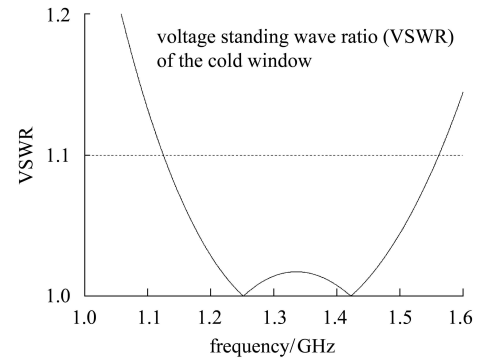


Fig. 4. Voltage standing wave ration of the cold window.

The optimized parameters are shown in Fig. 3. The windows part has a frequency bandwidth of 400 MHz with $\text{VSWR} < 1.1$ and a VSWR of 1.02 at 1.3 GHz. In other words, less than 2% RF power is reflected from the cold window, as shown in Fig. 4. The maximum surface electric field on the window is 8.5×10^{-2} kV/mm with 20 kW CW transmitted power, and the heat generation on the window is 7.7 W (set $\tan \delta = 5 \times 10^{-4}$). As the thermal conductivity of alumina in low temperature is about 60—

$100 \text{ W}/(\text{m}\cdot\text{K})^{[6]}$, the temperature difference on the whole window is within 3 K and the vacuum breakdown or ceramic crack is unlikely to happen.

3.3 Design of the support structure

As the inner conductor is divided into two parts and does not touch the windows, a new method should be applied to fix the coaxial lines. Holding rods are finally chosen and optimized for the sake of difficulties in manufacturing. Two metal rods are located along the axis at a 90 degree angle, as shown in Fig. 5. In view of the equivalent circuit, the current on the rods makes the magnetic field energy larger than the electric field energy, so the rods act as inductors L . Numerical calculations show that the RF property is related to the angle of the rods. That is to say there are electromagnetic interactions between the rods. We can use a mutual inductance M (determined by the angle and the distance of two rods) to describe it, as shown in Fig.6. By solving the equations we find that when $L = M \exp(id\beta)$, the magnetic field caused by mutual inductor can match those by

inductance, where d is the distance of the rods, β is the wave number.

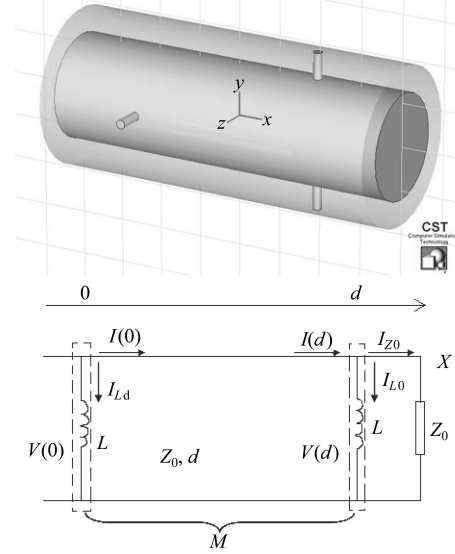


Fig. 5. Structure and equivalent circuit of the holding rods.

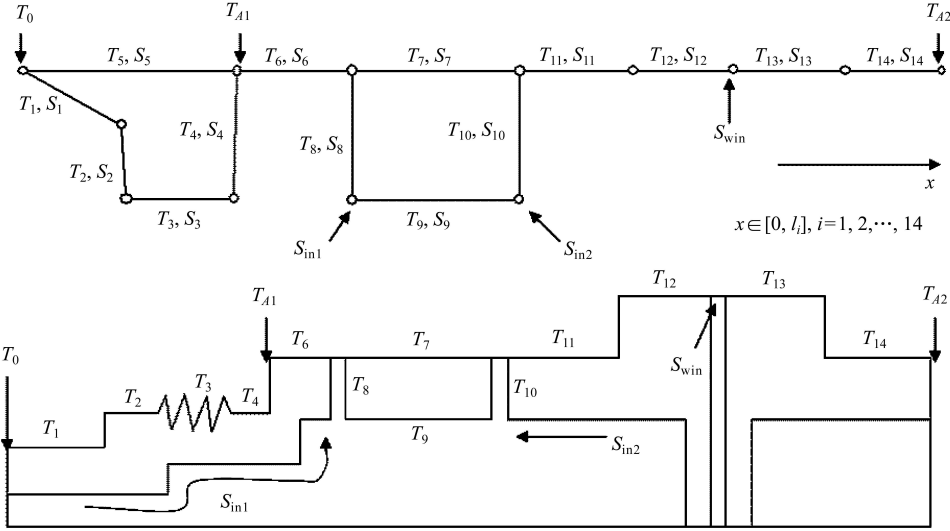


Fig. 6. Simplified one dimensional modal of the coupler structure.

After optimization, the diameter of holding rods is set to 4 mm to ensure the mechanical strength, and the distance of the rods is set to 77.4 mm. The structure has a frequency bandwidth of 80 MHz with $\text{VSWR} < 1.1$ and a 0.5% reflection energy at 1.3 GHz.

4 Thermal analysis

It is necessary to analyze the temperature distribution and the thermal flow in the coupler, because it is connected to the 2 K cryomodule and we should control the temperature on the cold window to pre-

vent it from breaking up. Most parts of the structure have axial symmetry, so we can simplify it as a one dimensional model, which is shown in Fig. 6.

In each part, the geometry, the electrical conductivity and the thermal conductivity can be treated as constant. We apply the thermal conduction equation to each part:

$$T_i''(x) = -\frac{S_i}{\lambda_i l_i A_i},$$

and the solution to the equation is

$$T_i(x) = a_i x + b_i - \frac{S_i}{2\lambda_i l_i A_i} x^2,$$

where $T_i(x)$ is the temperature distribution in the i -th part, S_i is the total heat generation, A_i is the area in the section which is vertical to the axially axes, l_i is the length of the part, λ_i is the thermal conducting coefficient, a_i and b_i are the unknown parameters. S_i can be obtained by calculating the surface loss in the electromagnetic field using Microwave Studio (MWS). We find that the heat generation is similar in the traveling wave and standing wave situations, and the cold window is located at the electrical field minimum, so S_i in the traveling wave is used to estimate the maximal temperature gradient. The temperature dependences of electrical and thermal conductivities are also taken into account. Applying the boundary conditions of temperature and energy, we set up a series of equations and solved the parameters a_i and b_i using Mathematica 5.

The temperature distribution on the ceramic discal window can be calculated as below: simplifying the window as a one dimensional modal and applying the thermal conduction equation to it, we get $T(r) = a \ln(r) + b$, where a and b are the unknown parameters, and r is the radius. The MWS results show that we can treat the heat generation on the window as a point source at $r_0 = 12$ mm, then the temperature at $r < r_0$ is constant. Applying the boundary conditions, we get:

$$T = \begin{cases} \frac{S_{\text{win}}}{2\pi\lambda d} \ln \frac{r_{\text{max}}}{r} + T_{13}(0), & r_0 < r < r_{\text{max}} \\ \frac{S_{\text{win}}}{2\pi\lambda d} \ln \frac{r_{\text{max}}}{r_0} + T_{13}(0), & r < r_0 \end{cases},$$

where $S_{\text{win}}=8.7$ W is the heat generation on the window, λ is the thermal conductivity of alumina (typically larger than $30 \text{ W}\cdot\text{m}^{-1}\cdot\text{K}^{-1}$ above $70 \text{ K}^{[6]}$), $d=3.6$ mm is the thickness of the window, $r_{\text{max}}=50$ mm is the radius of the window, and $T_{13}(0)$ is the temperature at r_{max} (see Fig. 6).

In the structure we set two thermal anchors of 78 K temperature (see Fig. 6, T_{A1} and T_{A2}). The calculation shows that at 20 kW transmitted power, the heat generation on the cold window is 7.8 W, which will cause a temperature difference of less than 20 K within the window, while on the edge of the window it is 170 K. The heat load to the LHe cryomodule is 1.2 W.

5 Conclusion

The capacitive coupling structure for the main coupler is demonstrated by theoretical analysis, and the geometries of the cold window, holding rods, other well-developed structures such as impedance transformer, “door-knob” and adjustable coupling antenna are optimized. A frequency bandwidth of 45 MHz with VSWR<1.1 is got.

The coupler is under fabrication at the factory. The follow-up works after the manufactory will include the tests on RF, vacuum and low temperature. A problem is that the heat load on LHe system may be too much, some additional modifications are necessary to reduce it to 0.5 W.

References

- 1 Garvey T. Physica C, 2006, **441**: 209
- 2 Matsumoto H, Kazakov S, Saito K. A New Design for a Super-Conducting Cavity Input Coupler. In: Horak C ed. Proceedings of the Particle Accelerator Conference. USA: Institute of Electrical and Electronics Engineers, Inc., 2005, 4141—4143
- 3 ZHU Feng, QUAN Sheng-Wen, JIAO Fei et al. High Power Laser and Particle Beams, 2006, **18**(4): 653 (in Chinese)
- 4 CHU Xiang-Qiang. The Electron Beam Transportation of PKU-FEL. Beijing: Peking University, 2005 (in Chinese)
- 5 Matsumoto H. High Power Coupler Issues in Normal Conducting and Superconducting Accelerator Applications. In: A. Luccio, W. MacKay ed. Proceeding of the 1999 Particle Accelerator Conference. USA: Institute of Electrical and Electronics Engineers, Inc., 1999, 536—540
- 6 Hasan Padamsee, Jens Knobloch, Tom Hays. RF Superconductivity for Accelerators. New York: John Wiley & Sons, Inc., 1998. 179—197, 415
- 7 ZHANG Ju-Xian. Journal of Vacuum Science and Technology (China), 2006, **26**(1): 77 (in Chinese)
- 8 David M Pozar. Microwave Engineering (second edition). United States of America: John Wiley & Sons, Inc., 1998. 56—86